

# Fabrication and characterization of Ag doped hydroxyapatite-polyvinyl alcohol composite nanofibers and its in vitro biological evaluations for bone tissue engineering applications

U. Anjaneyulu<sup>1</sup> · B. Priyadarshini<sup>1</sup> · A. Nirmala Grace<sup>2</sup> · U. Vijayalakshmi<sup>1</sup>

Received: 23 August 2016 / Accepted: 18 October 2016 / Published online: 31 October 2016  
© Springer Science+Business Media New York 2016

**Abstract** Electrospinning is one of the promising techniques to fabricate the nanofiber based scaffold for bone regeneration applications. In this study, firstly sol–gel method was employed to synthesize 5 % of Ag doped hydroxyapatite and also 10 wt% of polyvinyl alcohol solution was prepared for the electrospun process. For the first time, we have successfully fabricated the composite nanofibers in the combination of various concentration of Ag doped hydroxyapatite such as 1, 2, 3, and 5 wt% with polyvinyl alcohol solution. The developed Ag doped hydroxyapatite-polyvinyl alcohol composites were further characterized by Fourier transform infrared spectroscopy and powder-X-ray diffraction analysis to examine the characteristic functional groups and phase composition of Ag doped hydroxyapatite embedded into polyvinyl alcohol matrix. The uniform distribution of Ag doped hydroxyapatite in polyvinyl alcohol polymer with nanofiber diameter of 188–242 nm range was confirmed by high resolution transmission electron microscope and dynamic light scattering analysis, also the chemical/elemental composition was observed by scanning electron microscopy-energy dispersive spectroscopy analysis. The antibacterial

activity was evaluated for the fabricated Ag doped hydroxyapatite polyvinyl alcohol composite nanofibers by using *Staphylococcus aureus* (*S. aureus*) and *Escherichia coli* (*E. coli*) pathogens and the results demonstrated that *E. coli* exhibits excellent zone of inhibition than *S. aureus* due to its lesser cell wall thickness. The hemocompatibility study proves that the developed composite nanofibers are blood compatible and showed the hemolytic ratio of less than 5 %. In addition to this, in vitro bioactivity assessment was carried out for 7 days by immersing in simulated body fluid solution to generate the dense apatite layer on their surfaces which was further examined by X-ray diffraction and scanning electron microscopy-energy dispersive spectroscopy analysis. Hence, these electrospun fabricated Ag doped hydroxyapatite-polyvinyl alcohol composite nanofibers will acts as a potential scaffold material for tissue engineering applications.

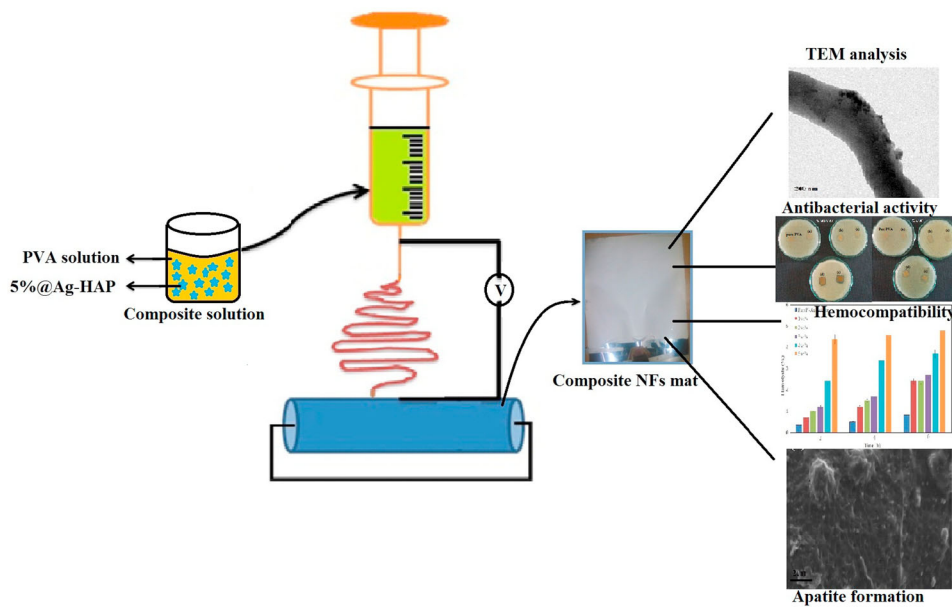
**Graphical Abstract** Graphical abstract of electrospun fabrication of Ag@HAP-PVA composite nanofibers and its in vitro biological evaluations.

---

✉ U. Vijayalakshmi  
vijayalakshmi.u@vit.ac.in  
lakesminat@yahoo.com

<sup>1</sup> Department of Chemistry, School of Advanced Sciences, VIT University, Vellore 632014 Tamil Nadu, India

<sup>2</sup> Center for Nanotechnology Research, VIT University, Vellore 632014 Tamil Nadu, India



**Keywords** Ag doped Hydroxyapatite · Electrospun nanofibers · Sol–gel synthesis · Antibacterial activity · Bioactivity · Bone tissue engineering

## 1 Introduction

Human bone is a complex system specially made of connective tissue and acts as a supporting appendage to the human body. Bone is very hard with superior mechanical strength in nature due to the combination of inorganic (Hydroxyapatite) and organic (Collagen) materials, which are embedded into the fibrous shaped extracellular matrix (ECM) [1, 2]. When bone undergoes the repair and damage by infection or accidental fractures, bone remodeling or regeneration can be accelerated with the adoption of autografts and allografts. These grafts have limitations to use in orthopaedic applications because of donor site morbidity and affect the immune system via transfer of pathogens to the human body from autografts and allografts respectively [3, 4]. To conquer these orthopaedic problems, recently electrospun nano to micro scale fibers are greatly implemented in tissue engineering applications to mimic the natural ECM with extraordinary properties including mechanical potency, cellular activation and enhanced osteoconductivity behavior owing to its large surface area to volume ratio and porosity [5, 6].

In the last few years, nanofibers based scaffold materials are greatly attracted towards tissue engineering applications due to its morphological and chemical structure similarity with natural bone system [7]. These nanofibers have several advantages in the field of biomedical area due to its high surface area to volume ratio with porous nature with

improved cell adhesion and differentiation, biocompatibility, biodegradability and mechanical strength etc [8]. Generally, these nanofibers are developed by using three different techniques such as phase separation, electrospinning and self assembly. However, among these methods electrospinning was highly suggested due to its easier handling, less expensive to fabricate the web like structure of nanofibers with diameter range from sub-micron to nano level [9, 10]. Hence, electrospinning fabricated nanofibers were drawn attention for biomedical engineering and played a vital role in drug delivery and wound healing applications [11, 12].

Hydroxyapatite [HAP:  $\text{Ca}_{10}(\text{PO}_4)_6(\text{OH})_2$ ] is a major constituent of natural bone and teeth, which is widely used in biomedical applications in the form of coatings on medical grade implants and bone substituent due to its exceptional properties such as biocompatibility, osteoconductivity, non-inflammatory and non-toxicity behavior with biological environment [13, 14]. However, HAP exhibits poor antibacterial performance and cause bacterial infections during the surgical treatment which leads to severe pain and results in the removal of ceramic materials from the body. In order to increase the bactericidal property of HAP, the incorporation of antimicrobial agents like  $\text{Ag}^+$ ,  $\text{Zn}^{+2}$ ,  $\text{Cu}^{+2}$  and  $\text{Ti}^{+4}$  have been made among all these metal ions  $\text{Ag}^+$  is highly recommended as dopant or substituent into the HAP crystal lattice owing to its excellent antibacterial ability and less toxicity at lower level concentrations [15, 16]. The combination of polymers such as chitosan, polyoxyethylene, polyvinyl alcohol, polylactic acid and polyacrylamide etc with hydroxyapatite as composites is suggested to improve the mechanical and functionality of nanofibers for tissue engineering applications. Among all these polymers,

polyvinyl alcohol (PVA) was selected because of its water soluble character, good thermal and chemical stability and also it contains the outstanding properties like biocompatible, biodegradable, non toxic and easier fiber forming nature. These properties of PVA were found to be used in wide range of applications such as cosmetic, medical, packaging and pharmaceutical applications [17, 18].

Sheikh et al. have synthesized PVA nanofibers with HAP nanoparticles and accomplished the investigation of apatite layer formation on the surface of nanofibers by immersion in SBF solution [19]. Kim et al. have developed the PVA–HAP composite nanofibers with improved thermal stability and proved that these nanofibers can acts as a promising material for hard tissue replacement and regeneration application [20]. Celebia et al. have prepared PVA-chitosan nanofibers by electrospinning method followed by the incorporation of Ag doped HAP to enhance the antibacterial activity against *E.coli* pathogens [21]. Suslu et al. have reported that the Ag doped HAP-poly (3-hydroxybutyrate-co-3-hydroxyvalerate: PHBV) composite nanofibers have good antibacterial activity and cytocompatibility for bone regeneration applications [22]. However, to the best of our knowledge no research reports have been existed on the fabrication of electrospun nanofibers with combination of PVA and various concentrations of Ag doped HAP to improve the biological properties. Therefore, in this present investigation we have developed composite nanofibers using PVA with various wt% of Ag@HAP powder such as 1, 2, 3, 4 and 5 %. The prepared composite nanofibers were characterized by FT-IR, XRD, SEM-EDAX, DLS and HR-TEM analysis. In addition to this, antibacterial activity, in vitro hemocompatibility and bioactivity studies were performed on the fabricated Ag doped HAP-PVA composite nanofibers to assess the significant characteristics of biomaterials for orthopedic and dental applications.

## 2 Experimental procedures

### 2.1 Materials

Polyvinyl alcohol: M.W 85, 000–1, 24, 000 SDFCL; silver nitrate: AgNO<sub>3</sub> Sigma Aldrich-99 %; phosphoric acid: H<sub>3</sub>PO<sub>4</sub> SDFCL-80 %; calcium nitrate tetrahydrate: Ca(NO<sub>3</sub>)<sub>2</sub>·4H<sub>2</sub>O-SDFCL; Aq. ammonia: Aq.NH<sub>3</sub> SDFCL-30 %; double distilled water: DD H<sub>2</sub>O; dimethyl sulphoxide: DMSO and phosphate buffer solution: PBS.

### 2.2 Sol–gel synthesized Ag doped HAP

The nanosized Ag doped HAP [Ca<sub>10-x</sub> Ag<sub>x</sub> (PO<sub>4</sub>)<sub>6</sub> (OH)<sub>2</sub>; x = 5 %] powder was synthesized by sol–gel method using 0.95 M of calcium nitrate tetrahydrate (Ca(NO<sub>3</sub>)<sub>2</sub>·4H<sub>2</sub>O)

and 0.6 M orthophosphoric acid (H<sub>3</sub>PO<sub>4</sub>) as calcium and phosphorus sources respectively. The silver nitrate (AgNO<sub>3</sub>) acts as dopant in the site of “Ca” and its concentration uphold at 0.05 M to maintain the ratio of Ca<sup>+</sup>Ag/P as 1.67. These source materials were dissolved in double distilled (DD) H<sub>2</sub>O and aqueous ammonia solution (NH<sub>3</sub>) was added to maintain the pH at 10. The developed white colored slurry was stirred for 2 h and aged it for 24 h at room temperature. The aged mixture was dried at 100 °C for 12 h and washed with DD H<sub>2</sub>O for several times to make aq. NH<sub>3</sub> free raw powder. The obtained raw powder was further sintered at 900 °C for 2 h to achieve the nano sized 5 % of Ag doped HAP (here after it is mentioned as Ag@HAP)\*.

### 2.3 Electrospinning process

In electrospun process, step wise methodology was adopted to fabricate the pure and composite nanofibers using colloidal solution containing 10 wt% of PVA with various concentrations of Ag@HAP (1, 2, 3, 4 and 5 wt%) and these composites ratios were shown in Table 1. Initially, 10 wt% aqueous solution of PVA was made by dissolving 1 g of PVA in 10 ml of DD H<sub>2</sub>O at 80 °C under vigorous stirring for 2 h. The synthesized Ag@HAP was added in different weight ratios such as 1, 2, 3, 4 and 5 wt% to the above prepared 10 wt% of PVA solution followed by stirred for 1 h to get a clear homogenous solution. The prepared Ag@HAP-PVA composite sol was aged for 12 h followed by sonification for 30 min. After this step, the developed sol was loaded into the plastic syringe (5 ml) and spin on the grounded alumina foil collector at a rate of 0.2 ml/h under the supply of 25 Kev at the distance of 15 cm. Finally, the obtained fiber mats were collected and dried in an oven for 24 h at 70 °C.

Further, the fabricated pure PVA and Ag@HAP-PVA composite nanofibers were analyzed by FTIR (SHIMADZU) to identify functional groups with the range of wavenumber from 4000 to 400 cm<sup>-1</sup>. The phase purity with respect to various compositions was found by powder XRD analysis using Cu Kα-1.5406 Å with step size of 0.02 Å° (Bruker D8 Advance) and surface morphology with

**Table 1** Theoretical values of composites solution preparation of Ag@HAP-PVA

S. No	Concentration of PVA (wt %)	Concentration of 5 % Ag@HAP (wt%)
1	10 (1 g/10 ml)	1 (0.1 g/10 ml)
2	10 (1 g/10 ml)	2 (0.2 g/10 ml)
3	10 (1 g/10 ml)	3 (0.3 g/10 ml)
4	10 (1 g/10 ml)	4 (0.4 g/10 ml)
5	10 (1 g/10 ml)	5 (0.5 g/10 ml)

elemental analysis was investigated using SEM-EDAX analysis (S4800 Hitachi). High resolution transmission electron microscope (HR-TEM; Tecnai, G2 20 Twin) was used to analyze the fiber mats which were made into small pieces and placed on Cu grid to characterize the internal morphology. The particle size was calculated by dynamic light scattering analysis (DLS), Ag@HAP powder and Ag@HAP-PVA composite nanofibers were dispersed in DD H<sub>2</sub>O by ultra sonification and determined their particle size using Horiba Nanoparticle (SZ-100).

## 2.4 Antibacterial activity

The qualitative zone of inhibition method was employed to examine the antibacterial activity of fabricated pure PVA and Ag@HAP-PVA composite nanofibers using two different microorganisms such as *Staphylococcus aureus* (*S. aureus*: gram positive) and *Escherichia coli* (*E. coli*: gram negative). Firstly, the pure PVA and Ag@HAP-PVA composite nanofibers were made into 1 × 1 cm size to perform the antimicrobial study. The mueller hinton agar medium acts as a growth factor for the microbes and medium was sterilized for further process, after sterilization the medium was poured into autoclaved petri plates and kept for 20 min under UV light. After this process, the microbe cell cultures were spread over on the surface using sterilized swabs. The pure and composite nanofiber mats were immersed in DMSO before placing on the agar medium for easier interaction with pathogens and also this organic solvent doesn't have any antibacterial activity. After completion of this process, the plates were incubated for 24 h at 37 °C followed by the zone of inhibition was measured in millimeter (mm) to analyze the bacterial inhibition of pure PVA and Ag@HAP-PVA composite nanofibers.

## 2.5 In vitro hemocompatibility study

The hemocompatibility study was assessed for the fabricated electrospun pure PVA and Ag@HAP-PVA composite nanofibers using human fresh blood which was obtained from healthy person. The acquired 5 ml of blood was mixed with PBS solution and centrifuged at 10,000 rpm for 3 min to separate the plasma from blood sample. After this step, 0.2 ml of blood was taken and mixed with 0.8 ml of PBS solution which contains the 1 × 1 cm of pure PVA and Ag@HAP-PVA composites nanofibers, which were incubated at 37 °C for 1 h in shaking conditions. The 0.2 ml of blood with 0.8 ml of DD H<sub>2</sub>O acts as positive control, whereas with PBS served as negative control. After incubation period, the blood with pure and composites nanofibers were centrifuged for 3 min at 10,000 rpm to collect the supernatant solution and readings were taken at 570 nm using BIORAD ELISA plate reader in a 96 well micro

titer plate. The blood compatibility of the pure and composites nanofibers was determined by using the following formula.

$$\text{Hemolytic percentage} = \frac{\text{Sample absorbance} - \text{negative control}}{\text{Positive control} - \text{negative control}} \times 100$$

## 2.6 In vitro bioactivity study

In vitro bioactivity study was performed by using simulated body fluid (SBF) solution which ionic composition and concentrations similar to the human physiological body fluid. The preparation of SBF solution was carried out according to the procedure suggested by Kokubo et al. [23] using various reagents such as NaCl (7.996 g), NaHCO<sub>3</sub> (0.350 g), KCl (0.224 g), K<sub>2</sub>HPO<sub>4</sub> (0.228), MgCl<sub>2</sub>·6H<sub>2</sub>O (0.305 g), CaCl<sub>2</sub> (0.278 g), Na<sub>2</sub>SO<sub>4</sub> (0.071 g) and C (CH<sub>2</sub>OH)<sub>3</sub>NH<sub>2</sub>·HCl (6.057 g). These chemicals were consequently added to 1 l of DD H<sub>2</sub>O and the pH of the solution was maintained at 7.35 ± 0.25 and kept at -4 °C in refrigerator. The electrospun pure PVA and Ag@HAP-PVA composite nanofibers with size of 1 × 1 cm were immersed in 15 ml of SBF solution for 7 days at 32 °C with subsequent refreshment of solution for every 24 h with fresh SBF solution to prevent the contamination. After SBF immersion, the composites nanofibers were observed by XRD and SEM-EDAX analysis to verify the bone like apatite layer formation on their surfaces.

## 3 Results and discussion

### 3.1 Fourier transform infrared spectroscopy (FT-IR)

FTIR spectrum (Fig. 1a) exhibits the characteristic absorption bands for PVA nano fiber at 3321 cm<sup>-1</sup> which corresponds to the stretching mode of OH-group, a band at 2952–2891 cm<sup>-1</sup> for the asymmetrical/symmetrical stretching mode of CH<sub>2</sub> group. It also exhibits the band at 1732 cm<sup>-1</sup> due to C=O band of partial acetate residual group present in the raw sample. The stretching C–H band at 1433–1252 cm<sup>-1</sup>, the stretching CO band of crystalline PVA at 1151 cm<sup>-1</sup>, the stretching CO band of amorphous PVA at 1096 cm<sup>-1</sup> and rocking CH bands at 847 cm<sup>-1</sup> were observed in the pure PVA polymer [24]. The Fig. 1b shows the absorption bands for 5 % of Ag doped HAP powder, the distinctive bands for PO<sub>4</sub><sup>3-</sup> group were observed at 1094, 1028, 968, 598 and 567 cm<sup>-1</sup>. The less intense bands were found at 636 and 3568 cm<sup>-1</sup> which corresponds to OH-group in hydroxyapatite crystal structure [25]. FT-IR spectrum from Fig. 1c–g belongs to various concentrations of 1, 2, 3, 4 and 5 wt% of electrospun composite nanofibers of Ag@HAP-PVA which demonstrate the characteristic bands for Ag doped HAP along with the PVA

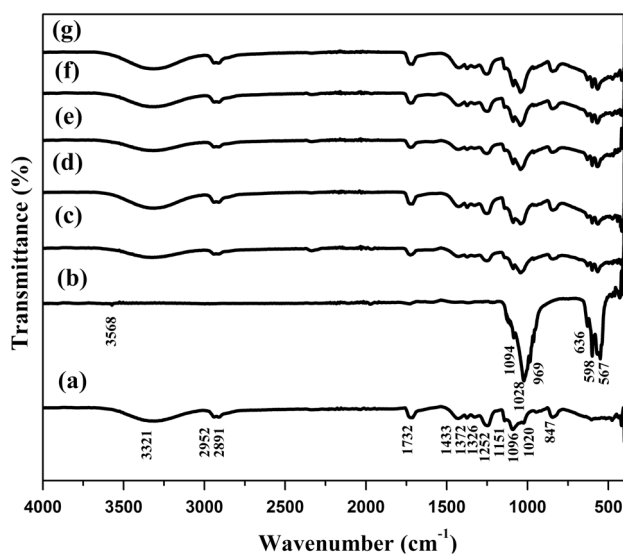


**Fig. 1** FT-IR spectroscopy of **a** pure PVA nanofiber, **b** Ag@HAP, **c** 1 wt% of Ag@HAP-PVA, **d** 2 wt% of Ag@HAP-PVA, **e** 3 wt% of Ag@HAP-PVA, **f** 4 wt% of Ag@HAP-PVA and **g** 5 wt% of Ag@HAP-PVA

material. The bands at 1094–969, 636–567  $\text{cm}^{-1}$  attribute the presence of Ag doped HAP and weak absorption bands detected at 3321, 2952–2891, 1732, 1433–1252, 1151, 847  $\text{cm}^{-1}$  which indicate the existence of PVA in composite nanofibers [26]. However, it was found that the FTIR bands at 1094–969 and 639–567  $\text{cm}^{-1}$  were slightly pronounced from 1 to 5 wt% of Ag doped HAP into PVA matrix due to increase in the addition of Ag@HAP. The band at 3568  $\text{cm}^{-1}$  was found to be disappeared in composite nanofibers due to the formation of strong hydrogen bonding between  $\text{OH}^-$  of Ag doped HAP and  $\text{OH}^-$  of PVA.

### 3.2 Powder-X-ray diffraction (XRD analysis)

The phase purity and composition of pure PVA and Ag@HAP-PVA composite nanofibers were determined by powder-XRD analysis. Figure 2a shows the XRD pattern of pure PVA nanofiber with broad peak position at 19.52° which indicates the semi crystalline nature of PVA. 2 $\theta$  from Fig. 2c–g correspond to the diffraction patterns of 1–5 wt% of Ag@HAP-PVA, it was found that those patterns exist the combination of diffract peaks for PVA at 19.52° along with the XRD patterns for the Ag@HAP. All the diffraction lines for HAP are found to exist at the 2 $\theta$  value of 25.92, 28.23, 29.03, 31.84, 32.24, 32.84 and 34.24° respectively. The Ag@HAP (Fig. 2b) peaks are exactly matched with standard pattern of HAP (JCPDS#9–432) without any other secondary phases such as  $\beta\text{-Ca}_3(\text{PO}_4)_2$  and AgO. However, from these XRD diffractograms we have found that the crystallinity of Ag@HAP increased from 1 to 5 wt% of composite nanofiber due to the increase in the inclusion of

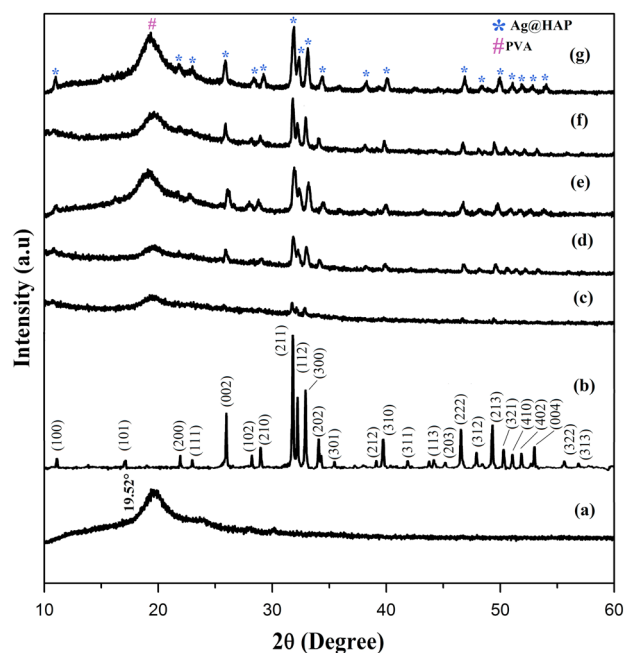


**Fig. 2** XRD patterns of **a** pure PVA nanofiber, **b** Ag@HAP, **c** 1 wt% of Ag@HAP-PVA, **d** 2 wt% of Ag@HAP-PVA, **e** 3 wt% of Ag@HAP-PVA, **f** 4 wt% of Ag@HAP-PVA and **g** 5 wt% of Ag@HAP-PVA

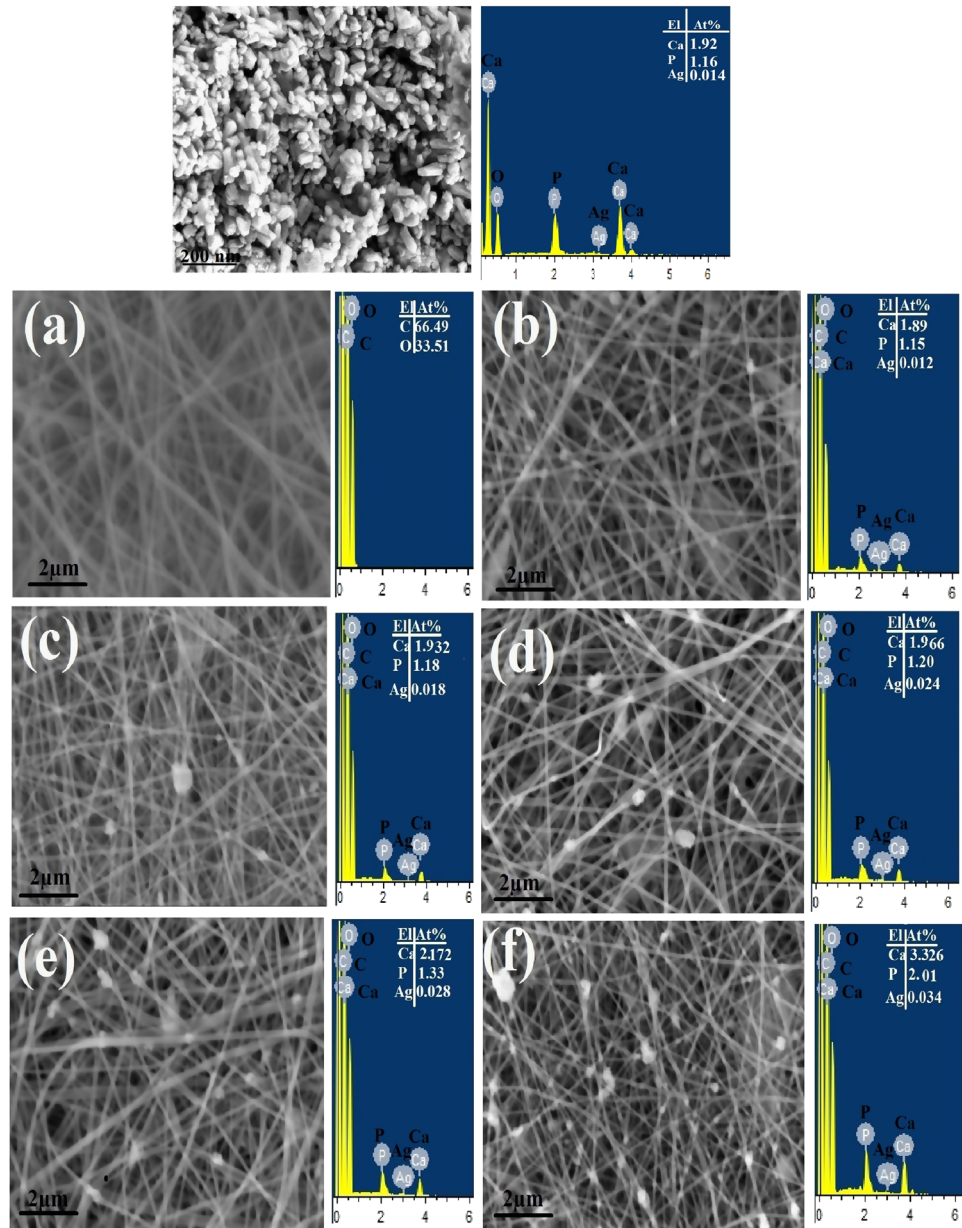
Ag doped HAP content into the PVA fiber. These XRD results were further proved by SEM-EDAX analysis.

### 3.3 Scanning electron microscopy-energy dispersive spectroscopy (SEM-EDAX)

The microstructural morphologies with elemental compositions of Ag@HAP, pure PVA and composite nanofibers were investigated by SEM-EDAX analysis. SEM micrograph of Ag@HAP (Fig. 3) was resembled as rod shaped morphology with highly agglomeration and size was in the range of nano to submicron. The elemental analysis of Ag@HAP was confirmed by EDAX spectrum and demonstrates the presence of Ca, P, O and Ag, which exhibits the Ca+Ag/P ratio as ~1.66. The SEM image represents in Fig. 3a corresponds to pure PVA nanofiber, which reveals that the fibers are of smooth surface with randomly oriented order and uniform with bead free formation. The length of the fibers was in micrometer to centimeter range and the diameter was in the range of nano to submicron range i.e 170 nm. The EDAX analysis confirms the presence of C and O elements in the pure PVA nanofibers mat. The composites nanofibers with combination of PVA with 1–5 wt% of Ag@HAP were shown in the Fig. 3b–f. The structural smooth surface of pure PVA nanofibers was changed by addition of various concentration of Ag@HAP. The Ag@HAP-PVA composite nanofibers were undergoing the minor destruction in the form



**Fig. 3** SEM-EDAX images of 5 % Ag doped HAP (Ag@HAP). SEM-EDAX analysis of **a** pure PVA nanofiber, **b** 1 wt% of Ag@HAP-PVA, **c** 2 wt% of Ag@HAP-PVA, **d** 3 wt% of Ag@HAP-PVA, **e** 4 wt% of Ag@HAP-PVA and **f** 5 wt% of Ag@HAP-PVA



of swelling the walls of fibers with non uniform manner because the PVA nanofibers were loaded with various concentrations of Ag@HAP nanoparticles. The average diameter of nanofibers was found to increase from 190 to 238 nm than the pure PVA nanofiber due to inclusion of agglomerated Ag@HAP nanoparticles into the PVA fiber. Also, the EDAX spectra confirms the existence of Ca, P, O and Ag elements in all the composite nanofibers, it was found that the ratio between Ca+Ag to P was between 1.65–1.67. From these EDAX spectra, we observed that the atomic percentages for Ca and P were gradually increased from 1 to 5 wt% of Ag@HAP-PVA composite nanofibers due to increase in the addition of Ag@HAP and which is correlated

with the theoretical values of Ag@HAP incorporation into PVA matrix.

### 3.4 High resolution-transmission electron microscopy (HR-TEM)

The HR-TEM image (Fig. 4) of Ag@HAP nanoparticles reveals the morphology as rod shape with agglomerated nature and particles were in the size of 184 nm which was confirmed by DLS analysis. Figure 4a shows the HR-TEM analysis of electrospun pure PVA and Ag@HAP-PVA composites nanofibers. As shown in TEM images (Fig. 4b–f), Ag doped HAP nanoparticles were uniformly

distributed in PVA matrix, whereas pure PVA nanofiber (Fig. 4a) are observed as plain and smooth in the interior of nanofibers. The amount of Ag@HAP nanoparticles increases with increase in the inclusion of nanoparticles into PVA matrix and also the diameter of nanofibers were found to be increased in the range of 188–242 nm which substantiate with SEM results and this was further proved by DLS analysis. Hence, HR-TEM images proved that 1–5 wt% of Ag@HAP were successfully embedded into the PVA matrix with appropriate allocation.

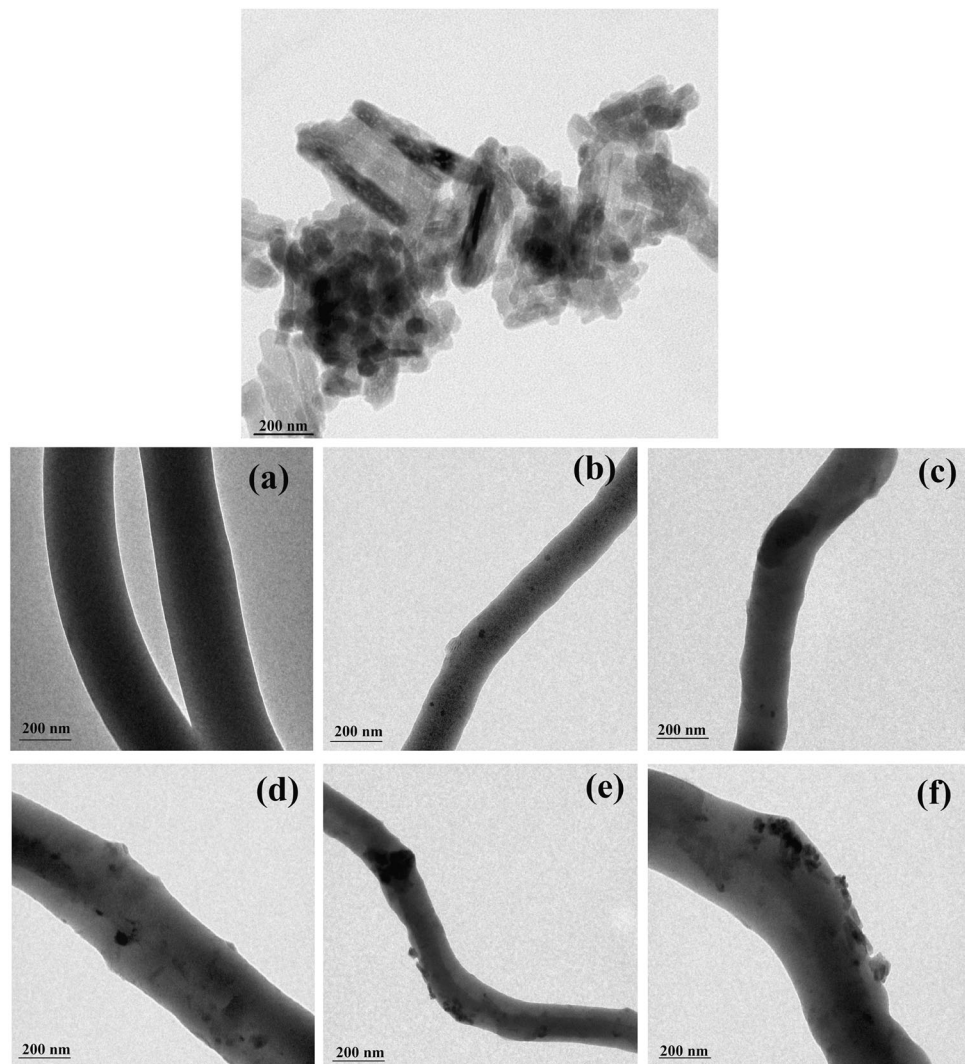
The average particle size distribution (PSD) was determined for Ag@HAP powder and 1–5 wt% of Ag@HAP in the PVA matrix using DLS analysis by dispersion in DD H<sub>2</sub>O, which was represented in Fig. 5. The particle size curve for Ag@HAP was shown in the Fig. 5a and its PSD value was observed as 168.6 nm. From Fig. 5b–f correspond to the PSD curves of 1, 2, 3, 4 and 5 wt% of Ag@HAP included in the PVA composites nanofibers and

which exhibit the average PSD values as 4.6, 8.2, 16.8, 21.4 and 49.2 nm respectively. Hence, this phenomenon of size increment was due to the aggregation of Ag@HAP nanoparticles in the PVA fiber with respect to increase in the addition of Ag@HAP from 1 to 5 wt%. This demonstrates that distribution of Ag@HAP particles within the PVA nanofiber and leads to increase of nanofiber diameter which corroborates with TEM analysis.

### 3.5 Antibacterial activity

The common infection causing pathogens such as *S. aureus* and *E. coli* were selected to examine the antibacterial activity of fabricated electrospun composite nanofibers. The antibacterial activity was evaluated in the form of zone of inhibition against *S. aureus* and *E. coli* for incubation of 24 h. The pure PVA and Ag@HAP-PVA composite nanofibers were made into 1 × 1 cm and placed on the pathogen spreads over

**Fig. 4** HR-TEM image of 5 % Ag doped HAP (Ag@HAP). HR-TEM images of **a** pure PVA nanofiber, **b** 1 wt% of Ag@HAP-PVA, **c** 2 wt% of Ag@HAP-PVA, **d** 3 wt% of Ag@HAP-PVA, **e** 4 wt% of Ag@HAP-PVA and **f** 5 wt% of Ag@HAP-PVA



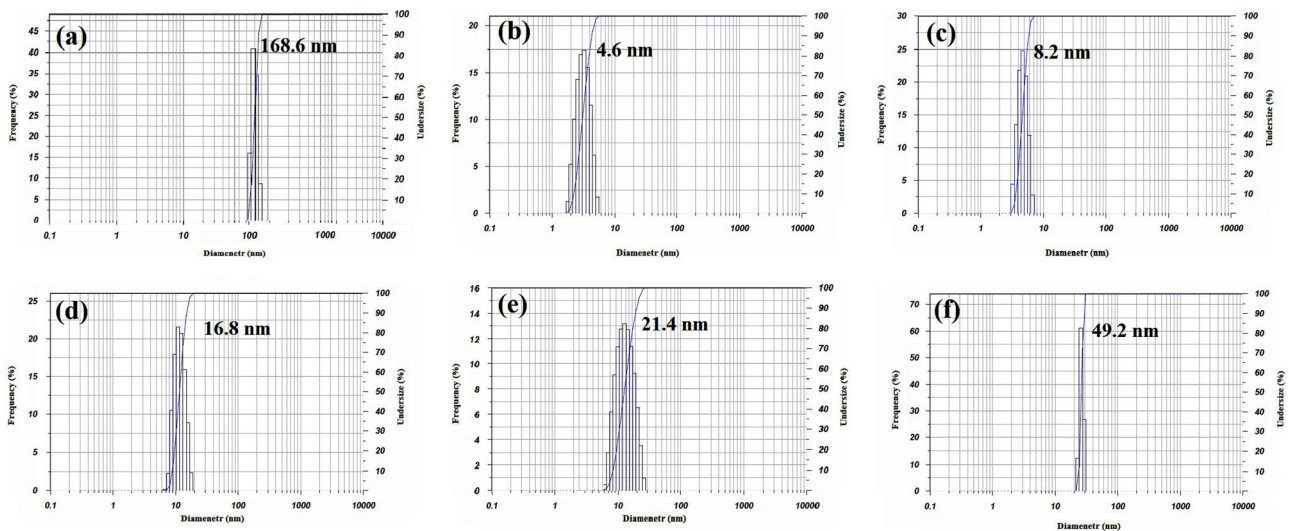


**Fig. 5** DLS analysis of **a** Ag@HAP, **b** 1 wt% of Ag@HAP-PVA, **c** 2 wt% of Ag@HAP-PVA, **d** 3 wt% of Ag@HAP-PVA, **e** 4 wt% of Ag@HAP-PVA and **f** 5 wt% of Ag@HAP-PVA

agar medium and placed in incubator, for the duration of 24 h and the obtained results were shown in Fig. 6. The bacterial restriction of pure PVA and composite nanofibers against *S. aureus* was shown in Fig. 6a. From these results, we confirmed that pure PVA mat exhibited no zone of inhibition whereas 1, 2, 3, 4 and 5 wt% of Ag@HAP incorporated PVA display the good zone of inhibition as 5, 7.5, 9.6, 10.4 and 12.2 mm respectively (Fig. 7). The antimicrobial behavior against *E. coli* illustrated in Fig. 6b, these images demonstrates that pure PVA is slightly exhibit the zone of inhibition (2 mm) and 1–5 wt% of Ag@HAP-PVA have shown excellent zone of inhibition as 8.2, 9.4, 11.2, 12.8 and 14.3 mm respectively (Fig. 7). These consequences concludes that *E. coli* have higher microorganism restriction ability than the *S. aureus* which might be due to the less denser cell wall and also the zone of inhibition was found to be enhanced with increase in the inclusion of Ag@HAP concentration into PVA matrix. However, these obtained results were correlated with the existed reports on Ag containing nanofibers and shown the improved microbial inhibition efficiency than the below mentioned reports. Tan et al. have evaluated antibacterial behavior of Ag NPs incorporated PVA nanofibers which exhibited the zone of inhibition from 6 to 12 mm for *E. coli*, *S. aureus*, *P. aeruginosa* and *B. megaterium* pathogens, also the bacterial restriction enhanced with increase in the addition of Ag NPs [27]. Calamak et al. have fabricated the Ag loaded silk nanofibers and examined its antibacterial activity against *S. aureus*, *S. epidermidis* and *P. aeruginosa* which shown the zone of inhibition as 8.3, 7.3 and 9.3 mm for glutaraldehyde treated nanofibers whereas 8.0, 8.3 and 8.6 mm for methanol treated nanofibers respectively [28]. Almajhdi et al. have developed the 0.1 and 7 wt% of Ag NPs with poly lactic-co

glycolic acid (PLGA) composite nanofibers and performed the disk diffusion method against *E. coli*, *S. aureus*, *B. cereus*, *L. monocytogenes* and *S. typhimurium*. In these nanofibers, 7 wt% of Ag/PLGA composites shows the good restriction behavior to the all pathogens with inhibition zone of 10 mm [29].

The mechanism of bacterial inhibition of 1–5 wt% of Ag@HAP-PVA is due to the release of  $\text{Ag}^+$  ions from composite nanofibers by degradation process and undergoes the electrostatic interaction with the pathogens. These  $\text{Ag}^+$  ions attack the cell wall membrane and leads to plasmolysis by cleavage of cell wall. Hence, these  $\text{Ag}^+$  ions undergo the penetration through cell membrane to disrupt the structure of DNA strands and cause the affect on respiration [30, 31]. Therefore, this antibacterial study reveals that the fabricated electrospun Ag@HAP-PVA composites nanofibers have excellent bacterial inhibition behavior towards *S. aureus* and *E. coli*. From the results we have concluded that these composite nanofibers are recommended to use in medical applications.

### 3.6 Hemocompatibility study

Hemolytic assay was performed on the biomaterials to determine their blood compatibility behavior in the human environment. In this study, we have evaluated the hemolytic percentage of pure PVA and Ag@HAP-PVA composite nanofibers by exposing the length of  $1 \times 1$  cm to human blood for 2, 4 and 6 h at 37 °C. According to, ASTM 756–00 and ISO 10993–5 1992 documents, the hemolytic index range less than 2 % is non hemolytic, 2–5 % is slightly hemolytic and greater than 5 % is hemolytic [32]. As shown



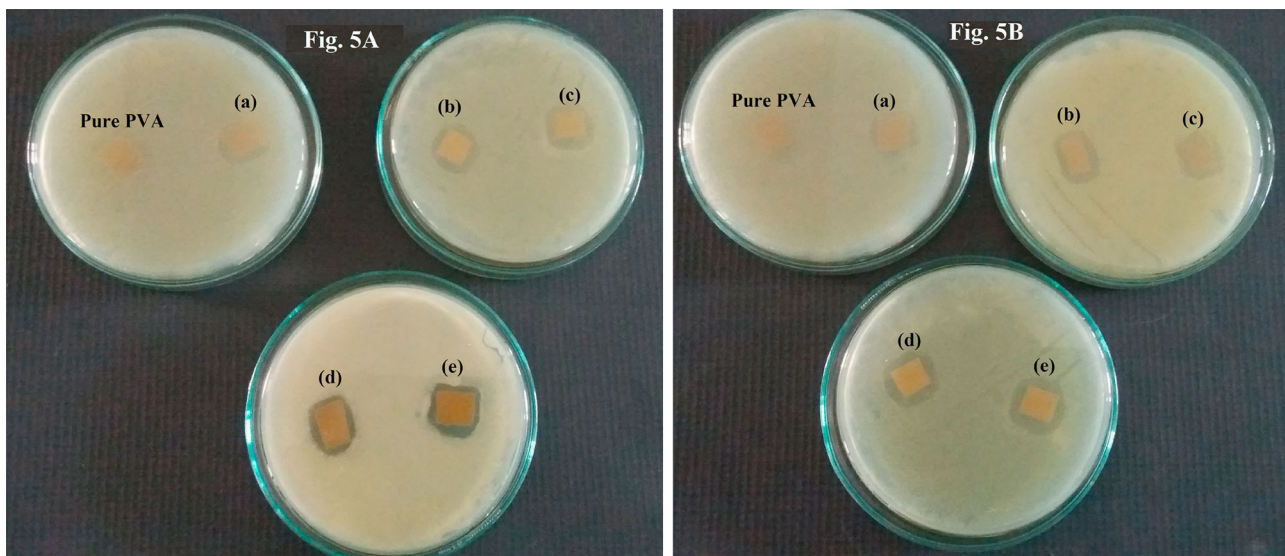


**Fig. 6** Zone of inhibition of **5a** *S.aureus* and **5b** *E.coli*, pure PVA nanofiber, **a** 1 wt% of Ag@HAP-PVA, **b** 2 wt% of Ag@HAP-PVA, **c** 3 wt% of Ag@HAP-PVA, **d** 4 wt% of Ag@HAP-PVA and **e** 5 wt% of Ag@HAP-PVA respectively

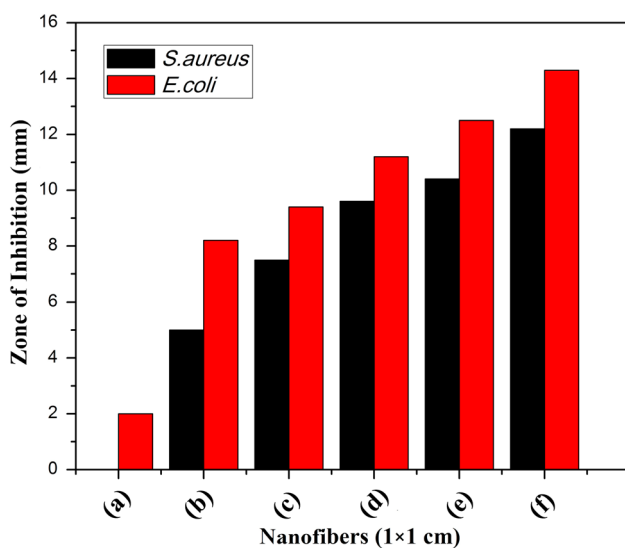


**Fig. 7** Zone of inhibition graph for the **a** pure PVA nanofiber, **b** 1 wt% of Ag@HAP-PVA, **c** 2 wt% of Ag@HAP-PVA, **d** 3 wt% of Ag@HAP-PVA, **e** 4 wt% of Ag@HAP-PVA and **f** 5 wt% of Ag@HAP-PVA against *S. aureus* and *E. coli*

in Fig. 8, the results indicated that the hemolysis ratio was found to increase from pure PVA to 5 wt% of Ag@HAP-PVA composite nanofiber with respect to increase the incubation periods from 2 to 6 h. The fabricated 1–3 wt% of Ag@HAP-PVA composite nanofibers have shown the hemolytic ratio of less than 2 % up to 4 h whereas at 6th h it have shown slightly hemolytic due to the release of Ag<sup>+</sup> ions from the nanofiber mat. However, 4 and 5 wt% of Ag@HAP incorporated PVA nanofibers exhibited moderate hemolytic

ratio between 2.4 and 4.9 % for 2–6 h due to the presence of higher amount of Ag ions. The increase in the hemolytic ratio from pure to composite nanofibers is due to release of Ag<sup>+</sup> ions from 1 to 5 wt% Ag@HAP-PVA composite fiber mats. The released Ag<sup>+</sup> ions interact with red blood cells which may lead to damage the erythrocyte membrane in terms of scrambling and shrinkage, and results in the release of intracellular hemoglobin. Hence, the fabricated 1–5 wt% of Ag@HAP-PVA composite nanofibers have shown the hemolytic ratio of less than 5 % and indicated that the composite nanofibers are safe to use as biomaterials for orthopedic applications. Furthermore, in vitro biocompatibility and in vivo animal studies are mandatory to assess the biological behavior of fabricated Ag@HAP-PVA composite nanofibers in clinical purposes.

### 3.7 In vitro apatite formation study

The SBF immersion test was used to determine the bone bonding ability of fabricated electrospun Ag@HAP-PVA composite nanofibers with natural bone by the formation of apatite layer on the surface of composite mats.

The XRD patterns of Ag@HAP-PVA composites nanofibers after 7 days of immersion in SBF solution was represented in Fig. 9. These SBF immersed XRD paradigms exhibited similar diffraction patterns when compared to the XRD spectra of HAP without SBF immersion. Further, it denotes that there was no change in the structural variation of HAP with no other secondary phases. The pure PVA nanofiber (Fig. 9a) diffraction peak intensity at  $2\theta = 19.52^\circ$  was found to be reduced when compared with before

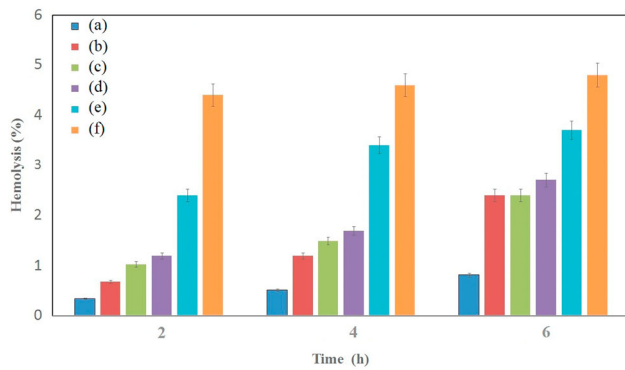


**Fig. 8** In vitro hemolytic assay of **a** Pure PVA nanofiber, **b** 1 wt% of Ag@HAP-PVA, **c** 2 wt% of Ag@HAP-PVA, **d** 3 wt% of Ag@HAP-PVA, **e** 4 wt% of Ag@HAP-PVA and **f** 5 wt% of Ag@HAP-PVA

immersion due to the degradation nature in SBF. Whereas, the diffraction peak of PVA in composites was completely disappeared after SBF immersion, this implies the rapid degradation in SBF solution because of combination with the resorbable calcium phosphate [33, 34]. However, from Fig. 9b–f it was observed that the composite nanofibers after immersion in SBF the HAP diffracted peaks were significantly become more pronounced and intensity of the peaks were sharpened when compared with before immersion. This behavior implies that enhancement in the crystallization of HAP structure in composites nanofibers owing to the dissolution and recrystallization process in SBF treatment [35, 36]. This was further evidenced by SEM-EDAX analysis.

Figure 10 shows the SEM-EDAX images of SBF immersed Ag@HAP-PVA composite nanofibers for 7 days at 37 °C. Figure 10a corresponds to pure PVA nanofiber which didn't show the apatite construction on the fibers and confirms the non-bioactive nature of polymer. Figure 10b–f images reveals that the bone like apatite layer formation on the surface of 1–5 wt% of Ag@HAP-PVA composite nanofibers are found to exist with irregular deposition and uniform porous network structure. As shown in the SEM images from Fig. 10b–f, the apatite mineral formation was found to be increased by the addition of 1–5 wt% of Ag@HAP content into the PVA matrix and also the porous nature was gradually disappeared in composite nanofiber mats with respect to higher concentration of silver. This phenomenon indicates that the Ag<sup>+</sup> ions plays vital role in the formation of apatite nuclei during the incubation of samples in SBF solution and confirms that higher content of Ag<sup>+</sup> in the composite nanofibers can able to accelerate the bone mineralization.

From these SEM images it can be clearly observed that the rate of apatite precipitation was more on the surface of 5 wt% of Ag@HAP-PVA composite nanofiber (Fig. 10f) and completely covered the fibers without any porous structures

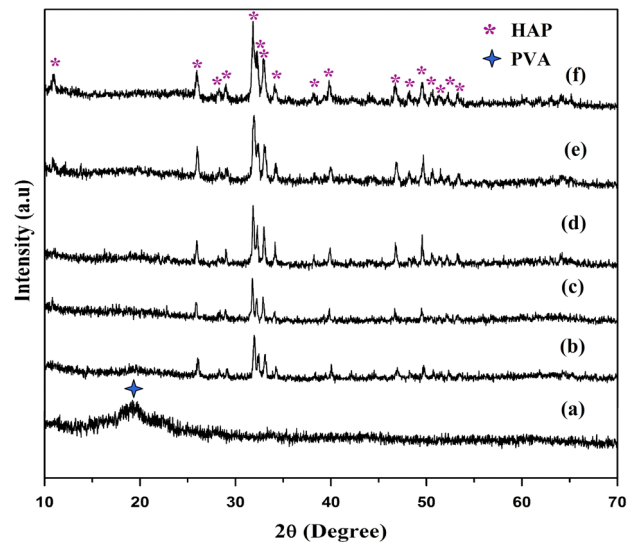


**Fig. 9** XRD patterns of **a** pure PVA nanofiber, **b** 1 wt% of Ag@HAP-PVA, **c** 2 wt% of Ag@HAP-PVA, **d** 3 wt% of Ag@HAP-PVA, **e** 4 wt% of Ag@HAP-PVA and **f** 5 wt% of Ag@HAP-PVA after immersion in SBF for 7 days

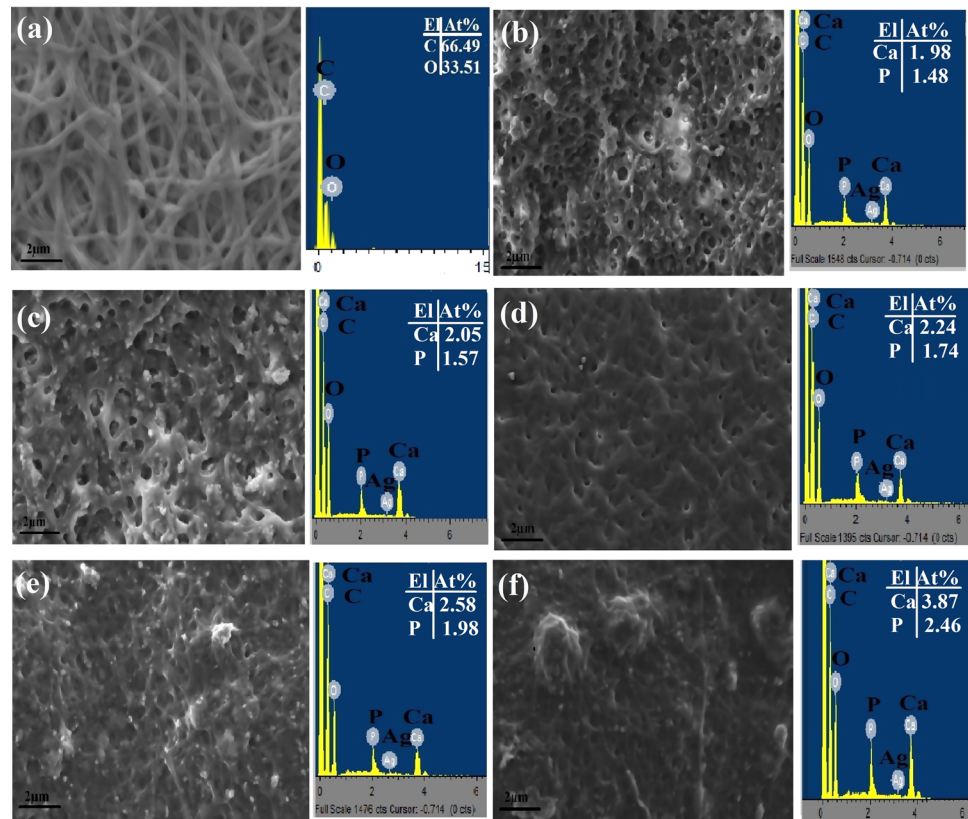
due to presence of high amount Ag @HAP powder in PVA matrix. The EDAX spectra confirms the existence of elements in the pure PVA and Ag@HAP-PVA composite nanofibers such as C, O and Ca, P, O, Ag respectively. However, the Ca and P atomic percentages was found to rise after SBF immersion for 7 days when compared with the non immersed EDAX spectra, which proves that formation of apatite layer on the surface of composite nanofibers at faster rate.

The mechanism of bioactive apatite layer formation was illustrated by number of research groups. Kokubo et al. [37] have reported that the surface functional groups of negatively charged ions influence the electrostatic attractions with SBF ions and induce the apatite nucleation. The OH-group of PVA can form the strong intermolecular hydrogen bonding with the OH<sup>-</sup> of Ag@HAP and PO<sub>4</sub><sup>3-</sup> of Ag@HAP was acts as the surface negative charges. This negative surface of Ag@HAP-PVA composite nanofiber initiates the apatite nucleation by attracting Ca<sup>2+</sup> ions from SBF solution and forms the Ca rich layer with positively charged surface. The developed Ca rich layer and Ag<sup>+</sup> ions can easily accumulate PO<sub>4</sub><sup>3-</sup> ions from SBF solution and leads to the formation of stable bonelike apatite [38].

## 4 Conclusions

In this present paper, for the first time we have successfully fabricated the electrospun composite nanofibers with the combination of 10 wt% of PVA and along with various concentrations of Ag@HAP such as 1, 2, 3, 4 and 5 wt%.

**Fig. 10** SEM-EDAX analysis of apatite formation on the surface of **a** Pure PVA nanofiber, **b** 1 wt% of Ag@HAP-PVA, **c** 2 wt% of Ag@HAP-PVA, **d** 3 wt% of Ag@HAP-PVA, **e** 4 wt% of Ag@HAP-PVA and **f** 5 wt% of Ag@HAP-PVA after immersion in SBF for 7 days



The following conclusions can be drawn from the above findings,

- The FT-IR and XRD analysis confirms that with increase in the concentration of Ag@HAP into the PVA matrix the crystallinity and the intensity of sharp bands for HAP at 1094–969, 639–567  $\text{cm}^{-1}$  are found to be increased.
- The SEM-EDAX and HR-TEM analysis reveals the surface morphology of composite nanofibers, which confirms that appropriate distribution of Ag@HAP nanoparticles into PVA matrix with diameter range from 188 to 242 nm. The DLS analysis confirms that the size of Ag@HAP nanoparticles were increased from 1 to 5 wt% composite nanofibers due to agglomeration and leads to enlarge the diameter of nanofibers.
- The antibacterial activity demonstrated that the fabricated 1–5 wt% of Ag@HAP-PVA composite nanofibers exhibits the excellent pathogen inhibition behavior towards *S. aureus* and *E. coli* respectively. However, the zone of inhibition for *E. coli* was found to be higher than *S. aureus* due to lesser thickness of cell wall.
- The hemocompatibility assay proves that the composites nanofiber have good compatible to the human blood with less than 5 % of hemolytic ratio. The bioactivity study reveals that the composite nanofibers are highly potential to develop the apatite layer formation on their surface

with increase in the concentration of Ag@HAP into PVA matrix.

Therefore, this investigation proved that the developed 1–5 wt% of Ag@HAP-PVA composites nanofibers can be successfully promote the rapid bone repair and regeneration in tissue engineering applications.

**Acknowledgments** One of the author U. Vijayalakshmi acknowledges the DST, New Delhi, India (SB/FT/CS-091/2012) for granting financial support. Also the authors express their gratitude to VIT University for providing all the research facilities.

#### Compliance with ethical standards

**Conflict of interest** The authors declare that they have no competing interests.

#### References

1. Song JH, Kim HE, Kim HW (2008) Electrospun fibrous web of collagen–apatite precipitated nanocomposite for bone regeneration. *J Mater Sci Mater Med* 19:2925–2932
2. Rho JY, Spearing LK, Zioupos P (1998) Mechanical properties and the hierarchical structure of bone. *Med Eng Phys* 20:92–102
3. Goldberg VM, Stevenson S (1987) Natural history of autografts and allografts. *Clin Orthop Relat Res* 225:7–16



4. Kaeding CC, Aros B, Pedroza A, Pifel E, Amendola A, Andrich JT, Wright RW (2011) Allograft versus autograft anterior cruciate ligament reconstruction. *Sports Health Multidiscip Approach* 3:73–81
5. Pascu EI, Stokes J, McGuinness GB (2013) Electrospun composites of PHBV, silk fibroin and nano-hydroxyapatite for bone tissue engineering. *Mater Sci Eng C* 33:4905–4916
6. Murugan R, Ramakrishna S (2005) Development of nano-composites for bone grafting. *Compos Sci Technol* 65:2385–2406
7. Leung V, Ko F (2011) Biomedical applications of nanofibers. *Polym Adv Technol* 22:350–365
8. Kanani AG, Bahrami SH (2010) Review on electrospun nanofibers scaffold and biomedical applications. *Trends Biomater Artif Organs* 24:93–115
9. Khang GS, Lee J, Kim MS, Lee HB (2006) In: Webster S (ed), *Biomaterials: tissue engineering and scaffold*. Wiley Press, New York
10. Chaignaud BE, Langer R, Vacanti JP (1997) In: Atala A and Mooney DJ (ed), *The history of tissue engineering using synthetic biodegradable polymer scaffolds and cells*. Birkhauser, Boston
11. Hong KH, Park JL, Sul IH, Youk JH, Kang TJ (2006) Preparation of antimicrobial poly(vinyl alcohol) nanofibers containing silver nanoparticles. *J Polym Sci B Polym Phys* 44:2468–2474
12. Hong KH, Kang TJ (2006) Hydraulic permeabilities of PET and nylon 6 electrospun fiber webs. *J Appl Polym Sci* 100:167–177
13. Anjaneyulu U, Pattanayak DK, Vijayalakshmi U (2016) Snail shell derived natural hydroxyapatite: Effects on Nih-3t3 cells for orthopedic applications. *Mater Manuf Process* 31:206–216
14. Anjaneyulu U, Pattanayak DK, Vijayalakshmi U (2015) The facile and phase pure evaluations of nano hydroxyapatite powder by sol-gel method. *Int J Chem Tech Res* 7:1516–1520
15. Iqbal N, Kadir MRA, Malek NANN, Mahmood NH, Murali MR, Kamarul T (2012) Rapid microwave assisted synthesis and characterization of nanosized silver-doped hydroxyapatite with antibacterial properties. *Mater Lett* 89:118–122
16. Archana R, Rakesh CB, Duraipandy N, Kiran MS, Deepak KP (2014) Synthesis, phase stability of hydroxyapatite-silver composite with antimicrobial activity and cytocompatibility. *Ceram Int* 40:10831–10838
17. Liao H, Qi R, Shen M, Cao X, Guo R, Zhang Y, Shi X (2011) Improved cellular response on multiwalled carbon nanotube-incorporated electrospun polyvinyl alcohol/chitosan nanofibrous scaffolds. *Colloids Surf B Biointerfaces* 84:528–535
18. Karim MR (2013) Fabrication of electrospun aligned nanofibers from conducting polyaniline copolymer/polyvinyl alcohol/chitosan oligosaccharide in aqueous solutions. *Synth Met* 178:34–37
19. Sheikh FA, Barakat NA, Kanjwal MA, Park SJ, Park DK, Kim HY (2010) Synthesis of poly(vinyl alcohol) (PVA) nanofibers incorporating hydroxyapatite nanoparticles as future implant materials. *Macromol Res* 18:59–66
20. Kim GM, Asran AS, Michler GH, Simon P, Kim JS (2008) Electrospun PVA/HAP nanocomposite nanofibers: biomimetics of mineralized hard tissues at a lower level of complexity. *Bioinsp Biomim* 3:046003
21. Celebia H, Gurbuz M, Kopal S, Dogan A (2013) Development of antibacterial electrospun chitosan/poly(vinyl alcohol) nanofibers containing silver ion-incorporated HAP nanoparticles. *Compos Interface* 20:799–812
22. Suslu A, Albayrak AZ, Bayir E, Urkmez AS, Cocen U (2015) In vitro biocompatibility and antibacterial activity of electrospun Ag doped HAp-PHBV composite nanofibers. *Int J Polym Mater* 64:465–473
23. Kokubo T, Kushitani H, Sakka S, Kitsugi T, Yamamuro T (1990) Solutions able to reproduce in vivo surface-structure changes in bioactive glass-ceramic A-W3. *J Biomed Mater Res* 24:721–734
24. Bahrami SH, Nouri M (2009) Chitosan-poly (vinyl alcohol) blend nanofibers: morphology, biological and antimicrobial properties. *E-Polymers* 9:1580–1591
25. Anjaneyulu U, Swaroop VK, Vijayalakshmi U (2016) Preparation and characterization of novel Ag doped hydroxyapatite-Fe<sub>3</sub>O<sub>4</sub>-chitosan hybrid composites and in vitro biological evaluations for orthopaedic applications. *RSC Adv* 6:10997–11007
26. Asran AS, Henning S, Michler GH (2010) Polyvinyl alcohol-collagen-hydroxyapatite biocomposite nanofibrous scaffold: mimicking the key features of natural bone at the nanoscale level. *Polymer* 51:868–876
27. Tan G, Saglam S, Emul E, Erdonmez D, Saglam N (2016) Synthesis and characterization of silver nanoparticles integrated in polyvinyl alcohol nanofibers for bionanotechnological applications. *Turk J Biol* 40:643–651
28. Calamak S, Aksoy EA, Ertas N, Erdogdu C, Sagiroglu M, Ulubayram K (2015) Ag/silk fibroin nanofibers: Effect of fibroin morphology on Ag<sup>+</sup> release and antibacterial activity. *Eur Polym J* 67:99–112
29. Almajhdi FN, Fouad H, Khalil KA, Awad HM, Mohamed SHS, Elsnaragaway T, Albarrag AM, Jassir FFA, Abdo HS (2014) In-vitro anticancer and antimicrobial activities of PLGA/silver nanofiber composites prepared by electrospinning. *J Mater Sci Mater Med* 25:1045–1053
30. Tank K (2014) *Nano hydroxyapatite and silver doped nano hydroxyapatite*. Scholar's Press, Mannheim, Germany
31. Tank KP, Chudasama KS, Thaker VS, Joshi MJ (2014) Pure and zinc doped nano-hydroxyapatite: Synthesis, characterization, antimicrobial and hemolytic studies. *J Cryst Growth* 401:474–479
32. Prodana M, Duta M, Ionita D, Bojin D, Stan MS, Dinischiotu A, Demetrescu I (2015) A new complex ceramic coating with carbon nanotubes, hydroxyapatite and TiO<sub>2</sub> nanotubes on Ti surface for biomedical applications. *Ceram Int* 4:16318–16325
33. Yusuf MK, Emily KC, John KK, Cato TL (2007) In situ synthesized ceramic-polymer composites for bone tissue engineering: bioactivity and degradation studies. *J Mater Sci* 42:4183–4190
34. Mabrouk M, Mostafa AA, Oudadesse H, Mahmoud AA, El Gohary MI (2014) Effect of ciprofloxacin incorporation in PVA and PVA bioactive glass composite scaffolds. *Ceram Int* 40:4833–4845
35. Lijun K, Yuan G, Guangyuan L, Yandao G, Nanming Z, Xiufang Z (2006) A study on the bioactivity of chitosan/nano-hydroxyapatite composite scaffolds for bone tissue engineering. *Eur Polym J* 42:3171–3179
36. Cziko M, Bogya ES, Barabas R, Bizo L, Stefan R (2013) In vitro biological activity comparison of some hydroxyapatite-based composite materials using simulated body fluid. *Cent Eur J Chem* 11:1583–1598
37. Kokubo T, Kim HM, Kawashita M (2003) Novel bioactive materials with different mechanical properties. *Biomaterials* 24:2161–2175
38. Gu YW, Khor KA, Cheang P (2004) Bone-like apatite layer formation on hydroxyapatite prepared by spark plasma sintering (SPS). *Biomaterials* 25:4127–4134